

Massive Stars in the Quintuplet Cluster

Donald F. Figer¹, Ian S. McLean¹, Mark Morris¹

ABSTRACT

We present near-infrared photometry and K-band spectra of newly-identified massive stars in the Quintuplet Cluster, one of the three massive clusters projected within 50 pc of the Galactic Center. We find that the cluster contains a variety of massive stars, including more unambiguously identified Wolf-Rayet stars than any cluster in the Galaxy, and over a dozen stars in earlier stages of evolution, i.e., LBV, Ofpe/WN9, and OB supergiants. One newly identified star is the second “Luminous Blue Variable” in the cluster, after the “Pistol Star.” While we are unable to provide certain spectral classifications for the five enigmatic Quintuplet-proper members, we tentatively propose that they are extremely dusty versions of the WC stars found elsewhere in the cluster, and similar to the dozen or so known examples in the Galaxy. Although the cluster parameters are uncertain because of photometric errors and uncertainties in stellar models, i.e., extrapolating initial masses and estimating ionizing fluxes, we have the following conclusions. Given the evolutionary stages of the identified stars, the cluster appears to be about 4 ± 1 Myr old, assuming coeval formation. The total mass in observed stars is $\sim 10^3 M_{\odot}$, and the implied mass is $\sim 10^4 M_{\odot}$, assuming a lower mass cutoff of $1 M_{\odot}$ and a Salpeter initial mass function. The implied mass density in stars is at least a few thousand $M_{\odot} \text{ pc}^{-3}$. The newly-identified stars increase the estimated ionizing flux from this cluster by about an order of magnitude with respect to earlier estimates, to $10^{50.9}$ photons s^{-1} , or roughly what is required to ionize the nearby “Sickle” HII region

¹University of California, Los Angeles, Division of Astronomy, Department of Physics & Astronomy, Los Angeles, CA 90095-1562

(G0.18–0.04). The total luminosity from the massive cluster stars is $\approx 10^{7.5} L_{\odot}$, enough to account for the heating of the nearby molecular cloud, M0.20–0.033. We propose a picture which integrates most of the major features in this part of the sky, excepting the non-thermal filaments. We compare the cluster to other young massive clusters and globular clusters, finding that it is unique in stellar content and age, except, perhaps, for the young cluster in the central parsec of the Galaxy. In addition, we find that the cluster is comparable to small “super star clusters.”

Subject headings: stars: supergiant — Galaxy: center — HII regions — open clusters and associations — ISM: individual (G0.15-0.05) — ISM: individual (G0.18-0.04)

1. Introduction

Three extraordinary bursts of star formation have produced young clusters in the Galactic Center (GC) in the past 10 Myr (Figer, Morris, & McLean 1996; hereafter FMM96; Krabbe et al. 1995; Nagata et al. 1995; Cotera et al. 1996; Serabyn, Shupe, & Figer 1998). In addition to their location in the Galaxy, these clusters are also special for being the most massive young clusters in our Galaxy. They offer us the possibility for investigating massive star formation in molecular clouds with extra-solar metallicity, large internal turbulent velocities, and strong magnetic fields. The many stars in each cluster may also finally provide the necessary statistics to investigate the existence of a true upper mass cutoff to the initial mass function (IMF) in the Galactic Center.

The Quintuplet Cluster is one of these massive clusters, and it is located approximately 30 pc, in projection, to the northeast of the Galactic Center (Glass, Catchpole, & Whitelock 1987). In addition to the five bright stars for which the Quintuplet was named (Nagata et al. 1990; Okuda et al. 1990), there is a clustering of hundreds of other stars in the vicinity. Our JHK' color composite (Figure 1) clearly shows a concentration of bright stars spanning a diameter of $\approx 50''$. Beyond this, cluster members are indistinguishable in continuum images from the already crowded field of stars in this part of the sky.

The cluster was originally observed as one or two sources in various infrared surveys (See §1 in Okuda et al. 1990 for a summary), until the late eighties, when three groups finally separated the cluster into a dozen or so sources (Nagata et al. 1990; Okuda et al. 1990; Glass, Moneti, & Moorwood 1990). Na-

gata et al. (1990) and Okuda et al. (1990) noted that 5 of the cluster stars are extraordinary in their large luminosities, very cool spectral energy distributions, and lack of intrinsic spectral features. They speculated that these objects might be young, dust-enshrouded stars.

Since then, many other cluster members have been identified as post main sequence descendants of O-stars (Moneti, Glass & Moorwood 1994; hereafter, MGM94; Geballe et al. 1994; Harris et al. 1994; Figer, McLean & Morris 1995; hereafter FMM95; FMM96; Cotera et al. 1996; Figer et al. 1998a). Most of these cluster stars are OB supergiants with strong winds, i.e, Wolf-Rayet stars, and LBVs. It is now clear that the Quintuplet Cluster is very massive, and that its members form a true physical group.

The Quintuplet Cluster is proving to be key in understanding answers to many important questions: 1) Is the cluster in the inner parsec of the Galaxy really “unique”, i.e., are extraordinary physical processes or continuous star formation scenarios required to explain the stellar content of the central cluster? 2) Do hot stars in the Quintuplet ionize the nearby H II regions, G0.18–0.04 (the “Sickle”) and G0.15–0.05 (the “Pistol”)? 3) Does the IMF in the Galactic Center favor the formation of high-mass stars? 4) Are stars in Quintuplet consistent with stellar evolution models which predict that WR/(WR+O) and WC/(WR+O) should be elevated in higher metallicity regions?

In this paper, we expand upon the work of FMM96 and Figer et al. (1998a) in showing that the Quintuplet Cluster is extraordinary for its membership of massive evolved stars. We present new JHK'nbL photometry (nbL is “narrow-band L”) and K-band spec-

trospectroscopy of the massive stars in the Quintuplet with the goal of answering some of the aforementioned questions. In §2, we describe the observations and data reduction. In §3, the spectral classifications are presented. We “sum” the properties of the individual stars in §4 to infer cluster properties, i.e., mass, age, and ionizing flux; the latter is used to argue that Quintuplet stars are ionizing the nearby HII regions. We compare the cluster properties to those of other massive clusters in the Galaxy and Magellanic Clouds in §5, arguing that it is a “near-twin” to the young cluster in the central parsec of the Galaxy (hereafter referred to as the “Central Cluster”), and is an older “brother” of the nearby Arches cluster. In this section, we present a consistent picture to account for the proximity of the Quintuplet, Pistol, and Sickie. We also interpret the Quintuplet Cluster as a “super star cluster,” i.e., those seen around other galaxies. Finally, in §6, we present conclusions, noting that the current sample of stars does not permit an investigation of the IMF or massive star evolutionary models. Such investigations await our HST/NICMOS data (Figer et al. 1998c)

2. Observations and Data Reduction

2.1. Observations

All data were taken with the UCLA double-beam near-infrared camera (McLean et al. 1993; McLean et al. 1994) at the University of California Observatories’ 3-m Shane telescope, producing a plate scale of $0''.7 \text{ pixel}^{-1}$. A grism was inserted into the beam, in conjunction with a 2-pixel wide slit mask, to produce spectra covering the K-band atmospheric window and having $R = \lambda/\Delta\lambda_{2\text{pix}} \approx 525$ (Figer 1995). Table 1 gives the identifications and coordinates for the target stars,

and the dates when the spectra were obtained. The numbering results from a count of stars in the July 20, 1994, K’-band image, proceeding from East to West and South to North. Stars #577 and #578 are located outside of this image, so they are numbered sequentially starting with the next integer after the last star in the image. Figure 1 is a JHK’ color composite of an $\approx 2''.8 \times 2''.8$ region centered on the cluster. Figures 2a-2d contain individual JHK’nbL images. Figure 3a shows an alternate greyscale stretch of the K’ image shown in Figure 2c at an expanded scale. Figure 3b gives a “zoomed” finder chart for the brightest cluster stars in Figure 3a which were included in the slit-scan data cube (see below).

2.2. Photometry

Photometry was extracted from two sets of images; the first set contains H- and K’-band images obtained on July 20, 1994, and the second set contains JHK’nbL images obtained on July 4, 1996. The seeing generally produced images with less than 2 pixels ($1''.4$) full-width at half maximum. The data were reduced according to the procedures in Figer (1995). In summary, bias structure and dark current were removed from target frames by subtracting “bias+dark” calibration frames; these images had the same exposure parameters as the target frames, except that an opaque mask was inserted into the beam when they were taken. Variations in system efficiency, especially due to pixel-to-pixel differences in quantum efficiency, were removed by dividing the target image by a “flat-field” image; these images were constructed by forming the median of a stack of frames, each taken with the telescope in a slightly different position. This “dithering” serves to eliminate objects in the final flat-field frame.

Final photometry was extracted using DAOPHOT, a point spread function-fitting routine in IRAF¹. Photometric apertures with 4''2 diameter were used, i.e., 3 times the size of the seeing disk. The results are listed in Table 2. K magnitudes were converted from K' using the relation in Wainscoat & Cowie (1992). We observed atmospheric standards from the list in Elias et al. (1982). The inferred zero-points from the July 4 images varied considerably as a function of time and airmass, i.e., the night was not photometric. We adopted the flux measurements in the first data set (Figer 1995), instead, for the H- and K-bands; the effective zero-points were estimated by minimizing the difference between the average photometry in the two data sets for the stars listed in Table 2. The J and nBL zero-points were extrapolated to high airmass from the observations of the standard stars. We assess a photometric error of ± 0.2 magnitudes for all bands.

2.3. Spectra

The spectra cover most of the K-band and were reduced using procedures described in Figer, McLean, & Najarro (1997). Some of the spectra were extracted from a slit-scan data cube covering a 1' (EW) \times 2' (NS) area, as shown in Figure 4. The telescope was stepped by 1'' along the east-west direction between exposures. Star #211 (Quintuplet star #3 according to MGM94) was used as an atmospheric standard in all cases. The observations presented in this paper, and those of others (Okuda et al. 1990; MGM94; Nagata,

Kobayashi, & Sato 1994; Figer et al. 1998b), show that #211 is spectroscopically featureless. The divided spectra were multiplied by a blackbody function, with $T = 630$ K, to correct for the intrinsic energy distribution of #211. We have found that this temperature is appropriate for the apparent K-band spectral energy distribution of #211 (see Figure 1 in Figer et al. 1998b). The spectra generally have $S/N \gtrsim 30$, i.e., features having $|EW| > 3 \text{ \AA}$ should be detectable at a level of a few times the noise in the continuum.

3. Spectral Classifications

Our spectral classifications are based upon K-band spectra. The final classifications are given in Table 3, along with the estimated luminosity and ionizing flux for each star. The Wolf-Rayet (WR) stars were classified using the atlas of Figer, McLean, & Najarro (1997; $R \approx 525$). Their montage of Galactic WR K-band spectra has been reproduced in Figure 5. The ‘‘OBI’’ stars were classified using the atlases of Hanson & Conti (1996) and Tamblin et al. (1996).

3.1. Wolf-Rayet Stars

Figure 5 shows that the emission lines for the Galactic WR stars tend to follow the expected trend of greater equivalent width for higher ionization species with earlier subtype. Spectral classification based upon K-band spectra is more effective in distinguishing different subtypes amongst the WN sequence than the WC sequence. WR108 (the only bona-fide WN9 star in the sample) lacks He II emission at $2.189 \mu\text{m}$, while WN8 stars show a hint of it. This is the strongest feature in earlier WN stars. This line, along with the $2.11 \mu\text{m}$ feature (He I/C III/N III), allows accurate discrimination to within 1 subtype for

¹IRAF is distributed by the National Optical Astronomy Observatories, which are operated by the Association of Universities for Research in Astronomy, Inc., under cooperative agreement with the National Science Foundation.

the WN sample in Figure 5 ($W_{2.189\mu\text{m}}/W_{2.11\mu\text{m}}$). The WC stars tend to have similar spectra except for the latest types (WC8 and WC9). This degeneracy can be partially lifted by measuring flux in the $3.09\mu\text{m}$ He II line (Figer 1995). WR112 and WR118 have featureless spectra, presumably due to dilution by dust emission (Williams, van der Hucht & Thé 1987).

The WR stars in our sample were classified by comparing their spectra (Figures 6a-6d) to the spectra in Figure 5 and by comparing their flux excesses at $3.09\mu\text{m}$ to those measured in Galactic WR stars. The newly identified WN9 stars in the Quintuplet Cluster, #256 and #274, have line widths similar to #320 (FMM95-1), and they lack He II emission ($2.189\mu\text{m}$). The new WN6 star, #353e, has prominent emission at $2.189\mu\text{m}$ which is comparable to the emission line strength near the $2.166\mu\text{m}$ He II line; it also has a considerable excess at $3.09\mu\text{m}$.

The new WC stars all have similar spectra, lacking the prominent emission at $2.058\mu\text{m}$ which is usually seen in WC9 stars, i.e., #76 (FMM95). Two of the stars, #309 and #235, are classified as earlier than WC8 for their excesses at $3.09\mu\text{m}$, while #151 has very little excess there. Together, the WN6 and the two “<WC8” stars are amongst the hottest identified stars within 50 pc of the Galactic Center, although their ionizing fluxes are quite meager owing to their small radii (Crowther & Smith 1996).

3.2. OB Supergiants

Spectra for the OB supergiants are shown in Figures 7-8. The “<B0I” stars have a featureless continuum, i.e., no features having $|EW| > 2\text{ \AA}$. Their K-band magnitudes put them in the supergiant class, and their fea-

tureless spectra are consistent with a classification earlier than B0I. Spectra for later types, i.e., A- or F- supergiants, have a relatively strong Brackett- γ line in absorption or emission (Hanson et al. 1996). All other OB supergiants were classified for the strengths of the three primary lines in the K-band: Brackett- γ ($2.166\mu\text{m}$), He I ($2.058\mu\text{m}$), and He I ($2.112/2.113\mu\text{m}$). The strength of the $2.058\mu\text{m}$ feature is suspect when there appears to be features near $2.312\mu\text{m}$ and $2.370\mu\text{m}$; all three features, when present, may be due to incomplete atmospheric correction. The “OBI” stars have Brackett- γ and He I ($2.058\mu\text{m}$) in emission with He I ($2.112/2.113\mu\text{m}$) in absorption; again, the $2.058\mu\text{m}$ line might be contaminated by improper atmospheric correction, as described above. The spectra are similar to those of HD 207329 (B1.5IB:e; Tamblyn et al. 1996) and BD+36 4063 (ON9.7Ia; Tamblyn et al. 1996 and Hanson & Conti 1996); it should be noted, though, that ON9.7Iab stars in Hanson & Conti (1996) have all three diagnostic features in absorption. Some Galactic Center stars also have similar spectra (c.f. IRS16NE, IRS16NW, and IRS33E in Genzel et al. 1996). The early BI stars were classified by measuring the equivalent widths in these three spectral lines, all in absorption, and comparing these values to those in the atlases. The Ofpe/WN9 stars have been previously classified (Geballe et al. 1994; Figer 1995; Cotera et al. 1996).

3.3. The Quintuplet-proper Members

The nature of the Quintuplet-proper members (QPMs) has remained a mystery since their discovery. They are very bright in the infrared, $m_K \approx 6$ to 9, and have cool apparent spectral energy distributions, i.e., infrared

color temperatures between ≈ 600 to 1,000 K. We present de-reddened SED's with blackbody fits in Figures 9a-d. The fits have been made to the data, dereddened by $A_K = 2.7$, instead of the higher value (see §4) derived for the other cluster stars; this has been arbitrarily done because the lower extinction value is better fit by a single-temperature blackbody. There is no a priori reason to expect that the emission should follow a single-temperature blackbody. In fact, the increased dereddened J-band flux that the stars would have if dereddened by $A_K = 3.2$ might be an indication of a rising spectrum for the underlying photosphere. We find good fits for temperatures of 780 K to 1,315 K. Glass et al. (1990) performed a similar analysis and found somewhat cooler temperatures due to the smaller extinction value they assumed. After dereddening, their integrated infrared luminosities are in the range $10^{4.3}$ to $10^{5.2} L_\odot$, yet no spectral features characteristic of supergiants have been found. In fact, the objects are spectroscopically featureless at all wavelengths observed, making their spectral classification ambiguous (Nagata et al. 1990; Okuda et al. 1990; Glass et al. 1990). Apparently, each object is composed of a powerful star(s) surrounded by dust.

Some have suggested that these objects are protostars, or at least not normal giants or supergiants (Okuda et al. 1990; Nagata et al. 1990; Glass et al. 1990); however, protostars would be much younger than the other stars identified in the cluster. In addition, protostars often emit polarized light, which is not the case for the QPMs (Nagata et al. 1994). Could they be OH/IR stars? Nagata et al. (1990) make strong arguments against this hypothesis, the strongest being that the stars do not have OH masers (Habing

et al. 1983; Winnberg et al. 1985; Sjouwerman 1998). In addition, OH/IR stars: 1) have deep water and CO absorption bands in their near-infrared spectra, 2) are less luminous than the QPMs, 3) are warmer than the QPMs, and 4) are much older than the QPMs, assuming that they are coeval with other cluster stars. Could they be red supergiant “monsters,” i.e., VY CMa? Such stars usually have SiO or water masers and deep water absorption features in the near-infrared. Could they be embedded OB stars? Again, this proposition has the same problem as the idea that they are protostars, i.e., such massive stars should have finished contracting and cleared away their circumstellar environment in much less than 1 Myr (Stahler 1994).

We suggest that these objects are dusty, late-type, WC stars (“DWCL”; c.f. Abbott & Conti 1987; Williams, van der Hucht & Thé 1987; Cohen 1995; FMM96). DWCL stars represent a short-lived phase of evolution when the coolest WC types (WC8 and WC9) tend to form dust shells. Williams, van der Hucht & Thé (1987) found that 19/27 of the WC8 and WC9 stars they studied have significant circumstellar dust emission which can be fit by blackbodies with temperatures of 780 K to 1,650 K (c.f., WR112 and WR118 in Figure 5).

To test this hypothesis, we have calculated apparent K-band magnitudes that various Galactic WC9 stars would have if they were in the Quintuplet. Despite their common luminosities of $\approx 10^5 L_\odot$, we find that m_K would span a very large range, ≈ 3 (WR112) to 12 (WR92). This is due to the different amounts of thermal emission from circumstellar dust around each star. The QPMs have apparent magnitudes in this range, $m_K \approx 6-9$. Of course, the range for DWCLs is so

large that this coincidence simply provides a consistency check, not a proof.

As another test of our hypothesis, we obtained J-band spectra of the QPMs so that the classical emission-line spectra might be seen. All known DWCLs begin showing the expected WCL emission-line spectrum in the J-band. We found no evidence for emission lines in the J-band spectra of these stars. Instead, we observed that the flux is still decreasing strongly with decreasing wavelength, as might be expected on the Wien side of a blackbody distribution. While this disagrees with the spectral energy distributions of all known DWCLs, note that such stars have all been found in surveys detecting their emission-line spectra. In other words, perhaps there are DWCLs which are completely enshrouded, i.e., their emission-line spectrum is not observable.

The nature of these stars is important for determining the WC/WN ratio in the cluster, a number which provides a crucial test of stellar evolution models (c.f. Meynet 1995). If they are DWCLs, then they are dustier than any others, begging the question: Is there something special about the Galactic Center environment, such as its high metallicity, which causes the winds of DWCLs to be particularly dusty? If they are not DWCLs, then they represent a new phenomenon. The same logic applies to the mid-infrared sources in the Central Cluster (Becklin et al. 1978). One possible avenue for further investigation is to concentrate on what is directly observable, i.e., the outer dust shell. We are pursuing this with high resolution mid-infrared imaging to measure the sizes of the dust shells as a function of wavelength for the QPMs and template DWCLs.

3.4. Luminous Blue Variables

Luminous Blue Variables (LBVs; Conti 1984) are rare stars in a presumably short phase of evolution between the main sequence and the Wolf-Rayet (WR) phase. They number about a half-dozen in the Galaxy and an equal number in the Magellanic Clouds. Given the similarities of the Central Cluster to the Quintuplet Cluster, it is perhaps no coincidence that both contain LBV or stars with LBV-like spectra (Tamblyn et al. 1996). FMM95 first identified the Pistol Star (#134) as an LBV candidate for its location in the HR diagram, near-infrared spectrum, and spatial proximity to the Pistol Nebula. They also suggested that the star ejected the gas now seen in the surrounding Pistol Nebula. Figier et al. (1998b) presented further near-infrared spectroscopy and photometry and applied wind-atmosphere and stellar evolution models to argue that the star is truly in an LBV stage.

Another cluster star, #362, appears to be luminous, hot, and photometrically variable. It brightened by +0.75 in the K-band while becoming redder by +0.34 magnitudes in H–K between the time when the two data sets were taken. The coincidence of the star becoming redder while also becoming brighter could be explained if it has a cool Mira-type companion. It is also possible that the star was moving to the red in the HR diagram, as LBVs often do when entering an eruptive stage. We favor the latter interpretation based upon our K-band spectrum (Figure 7a) which lacks CO absorption features expected from a Mira companion; the spectrum was obtained shortly after the star had brightened, so it should be a fair representation of the spectral energy distribution when the star was brighter. Note that such a large change

in H–K is equivalent to a change in effective temperature from $\geq 30,000$ K to $\sim 3,000$ K for normal stars. Although this range in temperature is rather large, it could be explained by the errors in the photometry. We assume that the fainter photometry is a better representation of the flux emitted by a hot photosphere, so we use it to estimate the luminosity assuming $BC_K = -1.5$, the “average” for the LBVs discussed in Blum, DePoy, & Sellgren (1995b).

3.5. Two nearby stars

We obtained K-band spectra and photometry for two stars within $5'$ (12.5 pc projected) of the Quintuplet which we suspect of being very young (Figure 10). The stars are N21 and N42 in the list of Nagata et al. (1993) and were selected because they fall to the red side of the reddening vector in a color-color plot, i.e., they are intrinsically red. We expected that they might be similar to the Quintuplet proper members. Integrating their spectral energy distributions gives $L \gtrsim 10^4 L_\odot$.

The two stars have nearly featureless spectra, except, perhaps, for emission at $2.06 \mu\text{m}$; this feature could be due to the He I line or incomplete cancellation of atmospheric absorption. We favor the first possibility, because the latter usually manifests itself as a combination of absorption and emission features, similar in appearance to P-Cygni profiles. N42 might have some weak emission features near $2.08 \mu\text{m}$ (C IV?) and $2.11 \mu\text{m}$ (C III). N21 appears to have absorption lines at $2.125 \mu\text{m}$, $2.182 \mu\text{m}$, and $2.315 \mu\text{m}$. The latter is most likely due to imperfect atmospheric correction. We do not have candidate transitions to associate with the other two lines. Both spectra are well-fit by cool blackbodies ($T \approx 2,000$ to $2,500$ K) after applying

dereddening to account for $A_K = 3.2$; however the extinction is not known. A larger assumed extinction would tend to produce a hotter energy distribution, but the dereddened spectra would then show an excessively high flux at shorter wavelengths. This is the expected effect in trying to deredden an intrinsically cool spectrum by assuming too much extinction.

The energy distributions and emission lines favor the possibility that these are hot stars embedded in dust. It is unclear if these stars were formed in the same or related star formation events. They might be outlying members of the Quintuplet Cluster, but it is difficult to determine without having velocities or ages for the stars.

4. Cluster Properties

In this section, we sum the individual contributions to the cluster properties in order to allow a comparison to other massive clusters and to determine whether the cluster is heating and ionizing nearby clouds and HII regions. For most parameters, we give the observed quantities as well as the implied values, assuming a Salpeter IMF (Salpeter 1955), and a particular lower mass cutoff as discussed below. Most of the estimates depend upon luminosities of the individual stars, so we start by estimating the extinction and distance.

4.1. Extinction

Figer et al. (1998b) reviewed extinction estimates to the cluster for their study of the Pistol Star, estimating $A_K = 3.28$. The estimate represents an average value inferred from color excesses of the stars in Table 1. Table 4 tabulates apparent colors and color excesses for the hot stars identified in the cluster. We consider two sample groups, the

“B1I–B3I” stars ($N = 5$), for which the spectral classifications are the most precise in the sample, and the “OBI” stars ($N = 9$); the latter includes the former. Although the “OBI” stars potentially span a larger range in subtype, i.e. O3–B9, they span a very narrow range in colors (c.f. Koornneef 1983), so we assume that all such stars have similar colors.

We use $A_K = 3.28 \pm 0.5$ ($A_V = 29 \pm 5$) throughout this paper, unless otherwise noted, where the error is the quadrature sum of the standard deviation of (H–K) for the full sample of OB supergiant stars in the cluster and the photometric errors. The variation in (H–K) for these stars is due to differences in the apparent colors of the stars, i.e., it is not due to inaccurate photometry or confusion. This can be seen in K-band spectra which show that $A_K = 3.28$ would overestimate the reddening to some of the stars, i.e., their dereddened energy distributions would be greater than that of an infinite temperature blackbody. We take this to indicate that there is some differential extinction across the field, and that an extinction value for each star will eventually have to be individually computed; however, the Quintuplet proper members are probably intrinsically very red. (We cannot estimate the true error in our estimate because it is dominated by systematic effects in the extinction law.)

4.2. Distance

We argue that the cluster is at the distance of the Galactic Center ($d_{GC} = 8,000$ pc; Reid 1993) for four reasons.

First, $V_{LOS} \approx 130$ km s⁻¹ for the cluster stars in every case where it has been measured (Figer 1995); this is also true for gas in the Pistol Nebula (Yusef-Zadeh, Morris, & van Gorkom 1989; Figer 1995; Lang et al.

1997). Such a high velocity is unlikely for objects along the line of sight to the Galactic Center, and a value of this magnitude is expected for an object with an orbital radius equal to the projected radius of the Quintuplet from the Galactic Center, i.e., $v_{orbital} = (GM/R)^{1/2} \approx 150$ km s⁻¹, where $M = 10^{8.2} M_{\odot}$ is the enclosed mass inside a 30 pc orbit (Sellgren et al. 1989).

Second, the Quintuplet Cluster appears to be ionizing the nearby “25 km s⁻¹ cloud” (M0.20–0.033; Lasenby, Lasenby, & Yusef-Zadeh 1989; Serabyn & Güsten 1991), thus creating the Sickie (Yusef-Zadeh & Morris 1987; Figer 1996; Lang et al. 1997). The particularly large line-widths associated with the molecular cloud are consistent with a location within the central molecular zone of the GC (Serabyn & Morris 1994).

Third, the inferred extinction (see above), interstellar polarization, and silicate absorption produced by the intervening interstellar medium to the cluster are consistent with a location at the GC (Okuda et al. 1990).

Lastly, components of the CO absorption bandhead at 4.66 μ m in the QPMs’ spectra have been attributed to the 250 pc ring (Okuda et al. 1990), due to their velocity shifts.

4.3. Luminosity

The total cluster luminosity can be estimated by summing the individual luminosities of the identified stars. This will provide a lower limit, because the cluster probably contains many unseen lower mass members; however, the total cluster luminosity should be dominated by massive stars for a reasonable IMF. We assumed a distance, extinction, and bolometric correction for each star, and tabulated the results in Table 3. It is impor-

tant to note that this estimate assumes that the cluster is coeval, and that the present-day masses are well-determined by the spectroscopic analysis above.

In order to estimate luminosities, we estimate the bolometric correction at K, $BC_K = M_{\text{BOL}} - M_K$. For the Ofpe/WN9 stars, we assume $BC_K = -2.9$ (Najarro et al. 1997). We assume $BC_K = -3.3$ for the WC stars and $BC_K = -2.9$ for the WN stars (Crowther & Smith 1996). We integrate the infrared flux for the DWCL stars. For the OB supergiant stars, we assume $BC_K = -2.0$. This is somewhat conservative compared to $BC_K = -2.4$, which is found by subtracting $V-K$ (Koornneef 1983) from BC_V for O9I stars (Vacca, Garmany, & Shull 1996); however, it allows for the fact that some of the OB supergiant stars will be later than late O type. For the LBVs, we assume $BC_K = -1.5$, according to the analysis of the Pistol Star by Figer et al. (1998b).

The total cluster luminosity is $10^{7.5} L_{\odot}$, counting all the stars in Table 3, and using the lower luminosity limit for the Pistol Star. Two of the most luminous stars in the cluster are LBVs, stars which span a very large range in BC_K ; but even without these two stars, we find $L_{\text{cluster}} = 10^{7.3} L_{\odot}$. Either value suggests that the Quintuplet Cluster is responsible for heating M0.20–0.033, which emits $10^7 L_{\odot}$ of radiation at infrared wavelengths (Morris, Davidson, & Werner 1995).

4.4. Mass

The total cluster mass cannot be directly estimated because the mass function has not been measured. The following analysis makes the assumption that the cluster has an IMF slope which is nearly Salpeter (Salpeter 1955). Note that measured IMF slopes vary consid-

erably about the Salpeter value (Scalo 1998).

We estimate the total cluster mass by counting the number of stars with initial masses between an assumed upper mass cutoff of $120 M_{\odot}$ and the lowest initial mass inferred from the list of stars identified in Table 1, $\approx 20 M_{\odot}$. Assuming 30 stars in this mass range, we calculate $M_{\text{cluster}} \approx 10^{4.2} M_{\odot}$ for $m_{\text{lower}} = 0.1 M_{\odot}$ and $10^{3.8} M_{\odot}$ for $m_{\text{lower}} = 1 M_{\odot}$.

We can compare this value to the mass required to ensure that the cluster is bound against tidal disruption. Assuming a circular orbit with a velocity equal to the line-of-sight velocity (130 km s^{-1} ; Figer 1995), and an orbital radius equal to the projected distance from the GC, we find an orbital time of ≈ 1.5 Myr. The enclosed mass at this radius is $\approx 10^{8.2} M_{\odot}$ (Sellgren et al. 1989). The condition for a star to be tidally bound at radius r_{cluster} is $M_{\text{total}} \gtrsim 2 \times M_{r < 30 \text{ pc}} \times (r_{\text{cluster}}/30 \text{ pc})^3 = 10^{4.1} M_{\odot}$, where r_{cluster} is the average distance of the stars in the table from the center of the cluster and is $\approx 1 \text{ pc}$. This value is on the same order as the values above, suggesting that the cluster is marginally bound against tidal disruption, at best.

4.5. Age

To estimate a single cluster age, we must assume that the cluster members in Table 1 are coeval. The notion of coevality is ambiguous when contraction timescales widely range, such as is the case when comparing high mass to low mass stars. We are not subject to this problem for the current analysis because we are concerned only with the massive stars, which all have very short contraction times (Stahler 1994).

Model isochrones from the Geneva models (Meynet et al. 1994) are shown in Figure 11 for twice solar metallicity and the “2×” \dot{M}

models. Data for the B supergiants in Table 1 have been overplotted. The stars have been given the same temperatures in light of their similar classifications, although note that the uncertainty in the spectral classifications is not represented in the error bar. Using lower metallicity or lower mass-loss rates will tend to give a higher age for the cluster, where the extreme value of 6 Myr is given by solar metallicity and the “standard” \dot{M} models.

The assumption of coevality is roughly consistent with the ages we estimate for the individual stars in Table 1 (Meynet 1995; and references therein). The presence of WC stars requires that the cluster is older than 2.5 Myr. The sole red supergiant requires an age $\gtrsim 4$ Myr (assuming $M_{\text{initial}} = 40 M_{\odot}$, “2 \times ” \dot{M} models, and $Z=0.04$). The Pistol Star requires an age of $\lesssim 2.1$ Myr, according to Figer et al. (1998b). The presence of OI stars requires an age between 2.5 and 4.7 Myr, depending on the mass-loss rates and the metallicity. We adopt an “average” age of 4 Myr for the cluster.

4.6. Ionizing Flux

Harris et al. (1994) estimate that the Sickle requires a Lyman continuum flux of $Q_{\text{Sickle}} \approx 10^{50.5} \text{ s}^{-1}$, and, according to Yusef-Zadeh et al. (1989), the Pistol requires $Q_{\text{Pistol}} \approx 10^{48.6} \text{ s}^{-1}$. Timmermann et al. (1996) use the radio flux at 32 GHz to estimate that the Quintuplet produces $Q_{\text{Quin, radio}} \approx 10^{50.2}/\eta \text{ s}^{-1}$, where η is less than 1 and accounts for dust absorption and deviations from an ionization-bounded region.

We find $Q_{\text{Quin, stars}} \approx 10^{50.9} \text{ s}^{-1}$ by summing the contributions from individual stars in Table 3. The OB stars presented here represent some of the previously predicted population of “unseen” hot stars (Harris et al.

1994; FMM95; Timmermann et al. 1996). While there may still be other O-stars with less pronounced spectral features in the cluster, i.e. those still on the main sequence, it appears that the presently identified hot stars produce enough ionizing radiation to ionize the gas in the Sickle, even though the geometry of the Sickle in relation to the cluster implies a covering fraction of $\approx 1/3$.

Figer et al. (1998b) give new estimates of the ionizing flux emitted by the Pistol Star spanning eight orders of magnitude (see their “L” and “H” models), demonstrating that it is highly dependent upon the exact physical parameters for the star. The range includes the ionizing flux required to ionize the Pistol Nebula, although contributions from other hot stars in the Quintuplet may be important, i.e., #151 (WC8) and #235 (<WC8).

5. The Quintuplet Cluster in Context

5.1. The Quintuplet Cluster compared to other massive clusters

Table 5 compares the Quintuplet Cluster and other massive clusters in mass, size, density, age, luminosity, and Lyman continuum flux. The total mass of observed stars, “M1,” is subject to observational effects, because of the varying distances of the clusters and the extent to which they have been studied. “M2” is supposed to represent the total inferred mass of the cluster; note that our estimates are for an IMF truncated below $1 M_{\odot}$. The radius is normally taken as the half-light radius, or average distance from the centroid of the cluster. Because of the slightly different definitions used in the estimates, the values should be taken as a rough indication of compactness; the same caution is obviously applicable to the resultant densities, “ $\rho 1$ ” and

“ $\rho 2$,” which are simply the mass estimates divided by the volume.

The Quintuplet Cluster is most comparable to NGC 3603 in mass and luminosity, but notice that it is much less dense, probably older, and produces less ionizing flux. Perhaps the differences in density and ionizing flux result from the difference in age, that is, the inevitable expansion of an unbound cluster, and the natural decrease of ionizing flux with age. The former effect might be amplified in the strong tidal field of the Galactic Center. Age might also be the reason for the large number of WR stars in the Quintuplet Cluster (8 to 13) compared to NGC 3603 (3, of the H-rich variety). In fact, the WR stars in NGC 3603 are probably hydrogen core burning O-stars with particularly thick winds, like those found in R136 (Massey & Hunter 1998); such stars are younger than “true,” i.e., He-burning, WR stars.

5.2. The Quintuplet Cluster and the Central Cluster

The emission-line stars in the central parsec of the Galaxy have been regarded as “exotic” for their spectral characteristics in the K-band (Allen, Hyland & Hillier 1990; Krabbe et al. 1991; Libonate et al. 1995; Krabbe et al. 1995; Blum et al. 1995; Tamblyn et al. 1996). While similar stars can be found in the Galaxy and the Large Magellanic cloud, they are rare and the ensemble of stars at the center, as a collection, is remarkable because it contains a concentration of such striking stars.

The Quintuplet Cluster contains similar stars, as can be seen in Figure 4 and FMM95. The WC9 stars found in the center (Blum, Sellgren & DePoy 1995; Krabbe et al. 1995) have counterparts in the Quintuplet Cluster

(here and FMM95-2); in fact, IRS6 in the Galactic Center is a particularly dusty WC9. IRS16NE, which has LBV-like spectral characteristics (Tamblyn et al. 1996), is similar to the Pistol Star, and #362. Some of the Ofpe/WN9 types in the center (IRS16 components) are similar to q8, q10 (Geballe et al. 1994; Figer 1995; Cotera et al. 1996), and FMM95-1. IRS33E, IRS16NE, and IRS16NW have spectra similar to the OB supergiant stars in the Quintuplet (Figer 1995; Najarro 1995; Genzel et al. 1996). IRS7, the red supergiant in the central cluster, is similar to q7 in the Quintuplet (Moneti, Glass & Moorwood 1994). Finally, the QPMs share similar spectral energy distributions (Okuda et al. 1990; Becklin et al. 1978) and K-band spectra (Figer 1995) with the very red sources in the Galactic Center, c.f. IRS8; both groups of stars may be dusty, late-type, WC stars (DWCLs).

In total, both clusters have approximately 27 supergiants, and contain roughly equal numbers of massive subtypes; therefore, the total mass in massive identified stars is the same in both clusters, $\approx 10^3 M_{\odot}$ (see Table 5). The small difference in total mass extrapolated down to m_{lower} is due to the different techniques used to make this estimate (see notes in Table 5 and Krabbe et al. 1995). The difference in “ $\rho 2$ ” is due to the difference in radius for the two clusters, but this is likely owed to a selection effect. The central cluster has been probed with very high resolution measurements, something which has not been done for the Quintuplet Cluster. Indeed, there appears to be a dense clustering of bright stars in the north-south ridge situated between the four westernmost QPMs and #211. Some of those stars have already been identified as being very massive, but

more identifications are limited by the spatial resolution of current observations. Further identifications in this stellar concentration would lower the effective radius for massive stars in the cluster. The collective luminosity and Lyman continuum flux for stars in each cluster are similar, where differences might be attributable to modeling.

In summary, the Quintuplet and Central cluster are nearly identical in mass and age. The primary difference seems to be the enigmatic broad helium-line stars in the Central Cluster (Krabbe et al. 1991). However, those stars are still evolved massive stars like the ones found in the Quintuplet Cluster, and the detailed line profiles in the Central Cluster stars are likely due to a small difference in age between stars in the two clusters (Najarro et al. 1997).

5.3. The Quintuplet, Pistol, Sickle complex

The center of the Quintuplet Cluster is situated $\approx 10''$ due north of G0.15–0.05 (the Pistol), and a few arcminutes to the southeast of G0.18–0.04 (the Sickle) (see Yusef-Zadeh & Morris 1987 for nomenclature). Serabyn & Güsten (1991) argued that the Sickle H II region is the ionized surface of M0.20–0.033 (the “25 km s⁻¹ molecular cloud”). Serabyn & Morris (1994) suggested that free electrons in the Sickle are accelerated by MHD interactions at this interface, and resultant relativistic electrons stream along nearby magnetic field lines, producing the non-thermal radio arcs. FMM95 suggested that the Pistol Nebula was ejected from, and is now partially ionized by, the Pistol Star.

The data in this paper are consistent with the hypothesis that the Quintuplet Cluster is heating dust in M0.20–0.033 and ionizing the

gas in the Sickle. M0.20–0.033 emits $\approx 10^7 L_{\odot}$ at far-infrared wavelengths (Morris et al. 1995), consistent with the idea that the Quintuplet Cluster and the molecular cloud are physically connected and not just coincident along the line of sight. Note that the large difference in velocities for the cluster and the cloud indicates that the cloud probably did not spawn the cluster.

Lang et al. (1997) presented radio recombination line data of both the Pistol and the Sickle showing that the former might be enhanced in helium, while the latter has solar helium abundance. Again, this is consistent with the idea that the molecular cloud is a wayward interloper in the region while the Pistol Nebula is composed of ejecta which has been subject to stellar nucleosynthesis. They also showed that ionized gas at the edges of the Sickle has been accelerated to higher velocities than that near the center of the nebula and the molecular gas in the cloud. We interpret this velocity field as indicating an interaction between the strong winds of the Quintuplet stars and the surface of M0.20–0.033. This agrees with Simpson et al. (1997) who suggest that the higher velocities come from a “champagne flow” interaction (also see Lang et al. 1997)

A nearby ring of emission at $l, b = (+0.15, -0.14)$ has been detected in mid-infrared data by the Midcourse Space Experiment (MSX; Shipman, Egan, & Price 1996). This ring appears to be associated with the complex, being coincident on its northwest portion with the Sickle (Egan et al. 1998). The cluster is offset from the center of the bubble, but such an offset might be explained by a relative motion of the Quintuplet Cluster and the local ISM, or to a large-scale density gradient in the medium into which the

bubble is expanding. Assuming that winds and radiation pressure from O-stars in the cluster have plowed the local ISM into a dust shell, we might expect a bubble expansion timescale of 10^4 yrs ($V_{\text{exp}} = 1,000 \text{ km s}^{-1}$). Such a timescale is more reasonable for a shell which was swept up by an expanding supernova shock front. Indeed, we expect 1 supernova per 50,000 yrs in the cluster, starting at a cluster age of ≈ 4 Myr according to Meynet (1995). A further analysis of this dust ring is under way using ISO data to investigate the excitation and kinematics (Levine et al. 1998).

5.4. The Quintuplet as a “Super Star Cluster”

Ho & Filippenko (1996; and references therein) argued that we are seeing present-day globular cluster formation in other galaxies. These super star clusters are recognized for their large luminosities, large masses, and compactness. Some have claimed that such clusters are produced in turbulent environments. Table 5 includes the physical characteristics of globular and super star clusters for comparison with the three Galactic Center clusters. The Quintuplet Cluster, Arches Cluster, and the Central Cluster are similar to the other objects compared in the table, except for their smaller mass, suggesting that they represent the low-mass end of the distribution of such objects.

If correct, then the GC clusters would be the closest examples of super star clusters. It would also add evidence that such clusters can form in galaxies which are not interacting. This might suggest a unified model for such phenomena. Perhaps super star clusters are formed wherever dense molecular clouds collide, or are strongly shocked, to form dense,

massive clusters. Such environments might be found in the early Galaxy and colliding galaxies, but they might also be found in the present-day Galactic Center. We speculate that the strength of the shock that provokes the cluster formation is the primary determinant of the cluster mass. In that case, the more violent encounters, such as those which occur in colliding galaxies, are the ones which would naturally produce the most massive clusters.

6. Conclusions

Although many of the parameters derived in this paper rely upon only near-infrared data, we conclude the following. The Quintuplet Cluster is extraordinary for its content of massive stars, containing more bona-fide Wolf Rayet stars than any other cluster in the Galaxy. It is the source of ionizing photons for the nearby H II regions, the “Pistol” and the “Sickle.” The types of stars found in the cluster are consistent with a coeval population, and the cluster age is $\approx 4 \pm 1$ Myr, according to stellar evolution models. The total mass in observed stars is $\sim 10^3 M_{\odot}$, and the inferred mass is $\sim 10^4 M_{\odot}$ for a Salpeter IMF and a lower mass cutoff in the range of $1 M_{\odot}$ to $0.1 M_{\odot}$. The observed mass density in stars is at least a few hundred $M_{\odot} \text{ pc}^{-3}$, and the inferred density is at least a few thousand $M_{\odot} \text{ pc}^{-3}$. The cluster is one of three massive clusters in the Galactic Center which are similar in many respects to super star clusters found in other galaxies. The current sample is limited to massive stars in various stages of post main sequence evolution and their initial masses are difficult to estimate. An accurate determination of the IMF in this cluster must await deeper observations (NICMOS/HST; Figer et al. 1998c) which will

reveal main sequence stars, where the association between infrared flux and initial mass is better known.

We thank the members of the Infrared Imaging Detector Laboratory at UCLA. We also thank Eric E. Becklin for useful discussions concerning the extinction to the Quintuplet Cluster. We thank Paul Crowther for stimulating discussions concerning BC_K and the ionizing fluxes of WR stars. We are very grateful to the referee, who provided many constructive comments which considerably improved the final manuscript. Finally, we thank Paco Najarro for pioneering the efforts to model massive stars in the Galactic Center.

TABLE 1
LOG OF SPECTROSCOPIC OBSERVATIONS

ID#	Nag90 ^a	MGM94 ^b	R.A. ^c	Dec. ^d		Dates Observed
				<i>s</i>	<i>'</i>	
76	5.1	49	11.6	July 26, 1994
134 ^e	...	seren	4.8	48	56.9	July 26, 1994
151	4.4	48	53.8	August 5, 1995
157	3.5	48	52.0	August 5, 1995
178	9.3	48	46.2	August 5, 1995
192	...	7	6.2	48	43.6	...
197	4.9	48	42.9	August 5, 1995
211 ^f	GCS4	3	5.5	48	39.0	...
231 ^g	GCS3-2	2	4.3	48	34.0	...
235	G	11a	4.8	48	33.5	August 5, 1995
240	...	8	5.5	48	31.2	...
241	F	10	4.7	48	30.2	August 5, 1995
242	4.1	48	30.0	August 5, 1995
243	GCS3-4	1	3.7	48	29.9	...
250	B	6	5.0	48	27.9	August 5, 1995, August 20, 1996
251	GCS3-1	4	4.4	48	27.6	...
252	4.1	48	27.1	August 5, 1995
256	6.1	48	25.2	August 5, 1995
257	D	13	4.8	48	25.5	August 5, 1995
258	GCS3-3	9	3.9	48	24.7	...
269	A	...	5.1	48	23.1	August 5, 1995
270N	C	5	4.7	48	21.3	August 5, 1995
270S	C	15	4.7	48	21.9	...
274 ^h	7.1	48	22.4	August 5, 1995
276	3.0	48	22.3	August 5, 1995
278	E	12	4.7	48	27.5	August 5, 1995
301	5.6	48	15.0	August 5, 1995, August 20, 1996
307	5.1	48	13.5	August 5, 1995, August 20, 1996
309	7.1	48	12.1	August 5, 1995
311	3.3	48	12.5	August 5, 1995, August 20, 1996
320	3.7	48	9.7	July 26, 1994
344	6.3	48	2.6	August 5, 1995, August 20, 1996
353E	0.8	47	58.3	August 3, 1995
358	6.2	47	58.2	August 5, 1995
362	7.6	47	56.6	August 20, 1996

TABLE 1—*Continued*

ID#	Nag90 ^a	MGM94 ^b	R.A. ^c	Dec. ^d		Dates Observed
				'	"	
381	3.1	47	52.2	August 5, 1995
406	3.5	47	43.5	August 5, 1995, August 20, 1996
577	53.8 ⁱ	51	41	July 5, 1996
578	57.8 ^j	48	47	July 5, 1996

^aNagata et al. (1990).

^bMoneti, Glass, & Moorwood (1994).

^cSeconds in right ascension offset from $17^h 43^m$.

^dMinutes and seconds of arc in declination from -28° .

^eThe “Pistol Star” (Figer et al. 1998b). “Pistol Source A” in Cotera et al. (1996). Object #25 in Nagata et al. (1993).

^fObject #26 in Nagata et al. (1993).

^gObject #24 in Nagata et al. (1993).

^h“Pistol Source B” in Cotera et al. (1996).

ⁱThis star falls outside of our K' -band image, so it does not have an identification number. Coordinates are for object #21 in Nagata et al. (1993). R.A. is in seconds of offset from $17^h 42^m$.

^jThis star falls outside of our K' -band image, so it does not have an identification number. Coordinates are for object #42 in Nagata et al. (1993). R.A. is in seconds of offset from $17^h 42^m$.

NOTE.—The Quintuplet-proper members have “GCS” designations in column 2. Coordinates are in equinox 1950.0 and are estimated from our images, based upon the coordinates for “q3” in Nagata et al. (1993). The “Dates Observed” column refers to when spectra were obtained.

TABLE 2
PHOTOMETRY

ID#	J	H1	H2	ΔH	K1	K2	ΔK	L	J-H	H1-K1	H2-K2	$\Delta(H-K)$	K-L
76	16.62	13.50	13.51	0.01	11.44	11.45	0.01	8.80	3.11	2.06	2.05	-0.00	2.65
134	12.08	9.08	9.33	0.25	7.14	7.39	0.24	5.93	2.75	1.94	1.94	0.00	1.45
151	17.54	13.29	13.39	0.10	10.41	10.47	0.06	8.21	4.15	2.88	2.92	0.04	2.26
157	12.81	11.81	11.73	-0.08	10.38	10.31	-0.07	...	1.08	1.43	1.42	-0.02	...
178	17.17	13.71	13.63	-0.08	11.86	11.84	-0.02	10.49	3.54	1.85	1.79	-0.05	1.35
192	13.39	...	9.68	7.74	...	6.33	3.71	...	1.94	...	1.41
197	...	14.23	13.66	0.57
211	15.11	10.67	10.68	0.01	7.66	7.12	-0.54	3.63	4.43	3.01	3.55	0.54	3.50
231	14.00	9.84	9.62	-0.21	...	6.27	...	2.96	4.37	...	3.35	...	3.32
235	14.41	11.21	11.44	0.23	9.40	9.79	0.39	8.44	2.97	1.80	1.65	-0.16	1.35
240	14.19	10.86	11.00	0.14	9.42	9.10	-0.32	7.81	3.19	1.44	1.90	0.46	1.29
241	13.57	10.61	10.60	-0.01	8.66	8.85	0.19	6.83	2.97	1.95	1.75	-0.20	2.02
242	14.85	12.61	12.63	0.02	10.44	10.88	0.44	8.70	2.22	2.17	1.75	-0.42	2.18
243	15.87	11.12	11.21	0.08	...	7.53	...	4.10	4.66	...	3.68	...	3.43
250	15.49	11.69	11.74	0.05	9.38	9.24	-0.14	6.89	3.75	2.32	2.50	0.19	2.35
251	14.67	10.54	10.78	0.24	...	7.61	...	4.66	3.89	...	3.17	...	2.95
252	...	13.05	9.72	3.33
256	14.77	11.93	11.99	0.06	10.40	10.37	-0.03	...	2.78	1.52	1.62	0.10	...
257	13.41	...	10.25	8.69	...	7.57	3.16	...	1.56	...	1.12
258	...	13.00	13.29	0.29	8.95	8.98	0.03	4.65	...	4.05	4.31	0.26	4.33
269	16.81	12.79	12.79	-0.01	10.68	10.67	-0.01	9.57	4.02	2.11	2.11	0.01	1.10
270N	14.62	...	10.75	7.81	...	5.50	3.87	...	2.94	...	2.31
270S
274	14.82	11.93	11.91	-0.03	10.41	10.42	0.01	9.06	2.92	1.52	1.49	-0.03	1.36
276	14.49	12.53	12.36	-0.17	10.80	10.82	0.01	9.97	2.13	1.73	1.54	-0.18	0.85
278	...	10.63	9.29	1.34
301	15.46	12.30	12.34	0.03	10.65	10.57	-0.08	9.39	3.13	1.65	1.76	0.11	1.18
307	13.92	10.81	11.03	0.22	9.38	9.31	-0.07	8.19	2.89	1.43	1.72	0.29	1.12
309	16.71	13.52	13.37	-0.15	11.60	11.44	-0.16	9.88	3.34	1.92	1.93	0.01	1.56
311	16.07	12.83	12.83	-0.01	11.12	11.11	-0.00	10.03	3.24	1.72	1.71	-0.00	1.09
320	15.58	12.44	12.35	-0.09	10.54	10.46	-0.08	8.97	3.23	1.90	1.89	-0.01	1.49
344	16.90	13.16	13.12	-0.04	11.32	11.23	-0.09	9.92	3.78	1.84	1.89	0.06	1.30
353E	...	13.12	11.53	1.59
358	15.98	12.27	12.37	0.10	10.29	10.26	-0.03	8.79	3.61	1.98	2.11	0.13	1.47
362	12.56	9.85	9.43	-0.41	7.99	7.23	-0.75	5.70	3.12	1.86	2.20	0.34	1.54
381	14.77	11.51	11.53	0.02	9.94	9.76	-0.18	8.48	3.24	1.56	1.77	0.20	1.28
406	15.97	12.87	12.69	-0.18	11.00	10.93	-0.07	9.74	3.28	1.87	1.76	-0.11	1.19

NOTE.—J, H2, K2, and L photometry are from the July 4, 1996, images. H1 and K1 photometry are from the July, 20, 1994, images. Zero-point magnitudes were determined by observing standard stars for the J, H1, K1, and L photometry. The zero-point magnitudes for the H2 and K2 photometry were set by minimizing ΔH and ΔK . K' photometry has been converted to K using the relation in Wainscoat & Cowie (1992). There has been no conversion between nbL and L. We assess an error of 0.2 magnitudes for all photometry.

TABLE 3
LUMINOSITY AND IONIZING FLUX ESTIMATES

ID#	Sp. Type	$\log(L/L_{\odot})^a$	$\log(N_{Ly,c})^b$	Refs. ^c
76	WC9	5.75	49.3	CS96
134	LBV	≥ 6.61	< 41.5	F98
151	WC8	6.15	49.7	CS96
157	$< B0I$	5.67	48.5	P73
192	M1a	4.90 ^d
211	DWCL?	4.84	48.7	BSD95
231	DWCL?	5.23	48.7	BSD95
235	$< WC8$	6.49	50.2	CS96
240	WN9/Ofpe	6.46	50.1	Na _j 94
241	WN9/Ofpe	6.66	50.3	Na _j 94
243	DWCL?	4.81	48.7	BSD95
250	$< B0I$	6.08	48.5	P73
251	DWCL?	4.61
256	WN9	6.01	49.5	CS96
257	B0I	...	48.5	P73
258	DWCL?	4.45	48.7	BSD95
269	OBI	5.54	48.5	VGS96
270N	late
270S	OBI	...	48.5	VGS96
274	WN9	6.00	49.5	CS96
276	B1I-B3I	5.48	46.2	P73
278	OBI	...	48.5	VGS96
301	$< B0I$	5.56	48.5	P73
307	B1.5Ia	6.07	46.5	P73
309	$< WC8$	5.72	49.4	CS96
311	B1I-B3I	5.36	46.2	P73
320	WN9	5.97	49.5	CS96
344	B1I-B3I	5.30	46.2	P73
353E	WN6	5.68	49.4	CS96
358	B1I-B3I	5.70	46.2	P73
362	OBI/LBVc	6.44 ^e	48.5	VGS96
381	OBI	5.86	48.5	VGS96

TABLE 3—*Continued*

ID#	Sp. Type	$\log(L/L_{\odot})^a$	$\log(N_{Ly,c})^b$	Refs. ^c
406	B1I-B3I	5.42	46.2	P73

^aThe luminosities were estimated assuming $d = 8,000$ pc, and $A_K = 3.28$. We assume BC_K of: -2.0 (OB supergiants), -3.3 (WC stars), -2.9 (WN and WN/Ofpe stars), -3.2 (#353E; Crowther & Smith 1996), and -1.5 (LBVs; Figer et al. 1998b). For the DWCLs, we integrated under the blackbody fits to the dereddened energy distributions. We assume $A_K = 2.7$ for the QPMs (see text).

^bIonizing fluxes have been taken directly from the references, except for the WR stars, where the following prescription has been used. $N_{Ly,c} = q_0 L / (\sigma T^4)$, where q_0 is taken from the reference, and is estimated as 24.9 for #353E, 23.6 for the WNL stars, 24.2 for the WC8 and WC9 stars, and 24.8 for the <WC8 stars; we assume temperatures of 55,000 K for #353E, 30,000 for the WNL stars, 42,000 K for the WC9 star, 48,500 for the WC8 star, and 55,000 K for the <WC8 stars.

^cReferences for ionizing flux estimate: BSD95, Blum, Sellgren & DePoy (1995); CS96, Crowther & Smith (1996); F98, Figer et al. (1998b); Har94, Harris et al. (1994); MGM94, Moneti, Glass & Moorwood (1994); Nag90, Nagata et al. (1990); Naj94, Najarro et al. (1994); P73, Panagia (1973); VGS96, Vacca, Garmany & Shull (1996).

^dWe assume BC_K of 2.60 for an average M supergiant.

^eThis estimate assumes the fainter photometry of July 20, 1994, and $BC_K = -1.5$, typical of LBVs, and very conservative for stars hotter than 20,000 K.

NOTE.—Spectral types, luminosities, and ionizing fluxes for the target stars. The total of the luminosities is $\log(L/L_{\odot}) = 7.50$, or 7.36 without the two LBV stars (#134 and #362). The total ionizing flux is $N_{Ly,c} = 50.9 \text{ s}^{-1}$.

A_K

TABLE 4

ESTIMATES FROM COLOR EXCESSES

	July 4, 1996 (J–H)	June 20, 1994 (H–K)	July 4, 1996 (H–K)	July 4, 1996 (K–L ^a)
(B1I–B3I) _{observed}	3.21	1.83	1.80	1.18
(B1I–B3I) _{intrinsic} ^b	–0.04	–0.03	–0.03	–0.07
E(B1I–B3I)	3.25	1.86	1.83	1.25
A_K ^c	3.40±0.60	3.30±0.18	3.26±0.34	3.01±0.50
OBI _{observed}	3.30	1.78	1.89	1.23
OBI _{intrinsic} ^b	–0.07	–0.04	–0.04	–0.07
E(OBI)	3.37	1.82	1.93	1.30
A_K ^c	3.53±1.21	3.23±0.38	3.43±1.12	3.13±1.04

^aThere has been no conversion between nbL and L.

^bValues were taken from Koornneef 1983.

^cAssumes the extinction law of Rieke, Rieke, & Paul (1989), i.e., $A_J/A_K = 2.73$, $A_H/A_K = 1.56$, and $A_L/A_K = 0.59$.

NOTE.—The extinction has been inferred from measured color excesses for the early B supergiants alone and for the wider, and inclusive, sample of all OB supergiants. The B1I–B3I stars are: #276, #311, #344, #358, and #406. The “OBI” sample contains all of the B supergiants listed above and: #269, #278, #362, and #381. The dates indicate when the measurements were made: note that there are two determinations of H–K taken from two different nights. The unweighted average of all estimates is $A_K = 3.28 \pm 0.16$. The weighted average is 3.27 ± 0.06 . Note that the quoted statistical errors are likely less than systematic errors due to uncertainty in the zero-points and the extinction law.

TABLE 5
PROPERTIES OF MASSIVE CLUSTERS

Cluster	Log(M1) M_{\odot}	Log(M2) M_{\odot}	Radius pc	Log($\rho 1$) $M_{\odot} \text{ pc}^{-3}$	Log($\rho 2$) $M_{\odot} \text{ pc}^{-3}$	Age Myr	Log(L) L_{\odot}	Log(Q) s^{-1}
Quintuplet	3.0	3.8	1.0	2.4	3.2	3–6	7.5	50.9
Arches ^a	3.7	4.3	0.19	5.2	5.8	1–2	8.0	51.0
Center ^b	3.0	4.0	0.23	4.6	5.6	3–7	7.3	50.5
NGC 3603 ^c	3.1	3.7	0.23	4.3	5.0	2.5	7.3	51.1
Trapezium ^d	1.5	...	0.05	4.7	...	0.3	≈ 5	48.9
R136 ^e	3.4	4.5	1.6	2.2	3.3	<1–2	>7.6	51.9
small globular (M5) ^f	...	4.8	4.0	...	2.3
typical globular (M13) ^f	...	5.5	3.9	...	3.1
large globular (M22) ^f	...	6.8	3.2	...	4.7
NGC 1705-1 ^g	...	4.9	0.9	...	4.4	10–20
NGC 1569-A ^g	...	5.5	1.9	...	4.0	10–20

^aSerabyn, Shupe, & Figer (1998).

^bKrabbe et al. (1995). The mass, “M2” has been estimated by assuming that a total $10^{3.5}$ stars have been formed. The age spans a range covering an initial starburst, followed by an exponential decay in the star formation rate.

^cDrissen et al. (1995). “M1” was estimated by assuming that the 37 stars in Table 3 of Moffat, Drissen, & Shara (1994) have $15 < M_{\text{initial}} < 120 M_{\odot}$. The “size” is the average projected radius for the stars in Table 3. The “age” is estimated by assuming that there are true helium-burning Wolf-Rayet stars in the cluster. See Eisenhauer et al. (1998) for an alternate interpretation. The luminosity has been estimated by assuming that the stars in Table 3 have an average luminosity of $10^{5.7} L_{\odot}$.

^dMcCaughrean & Stauffer (1994). The “radius” comes from the region which was probed with deep infrared imaging. “ $\rho 2$ ” is the stellar number density, i.e., it represents the mass density if the average mass per star is $1 M_{\odot}$. This number has been corrected for projection effects, i.e., volume number density $\approx 2 \times$ surface number density. “Q” is from Kennicutt 1984.

^eMassey & Hunter (1998). “M1” is a count of the total mass of the 29 stars in Table 3 of Massey & Hunter, using the Chlewbowski & Garmany (1991) calibration ($56 M_{\odot} < M_{\text{initial}} < 136 M_{\odot}$). The age corresponds to the young population of high mass stars. “Q” is from Walborn 1991.

^fAllen (1973).

^gHo & Filippenko (1996). The masses, “M2,” are inferred by measuring velocity dispersions and invoking the virial theorem.

NOTE.— “M1” is the total cluster mass in observed stars. “M2” is the total cluster mass in all stars extrapolated down to a lower-mass cutoff of $1 M_{\odot}$, assuming a Salpeter IMF slope and an upper mass cutoff of $120 M_{\odot}$ (unless otherwise noted); note that the total cluster mass would be 2.5 times greater if the lower mass cutoff is $0.1 M_{\odot}$. “Radius” gives the average projected separation from the centroid position. “ $\rho 1$ ” is M1 divided by the volume. “ $\rho 2$ ” is M2 divided by the volume. In either case, this is probably closer to the central density than the average density because the mass is for the whole cluster while the radius is the average projected radius. “Age” is the assumed age for the cluster. “Luminosity” gives the total measured luminosity for observed stars. “Q” is the estimated Lyman continuum flux emitted by the cluster.

REFERENCES

- Abbott, D. C. & Conti, P. S. 1987, *ARA&A*, 25, 113
- Allen, C. W., 1973, in *Astrophysical Quantities*, 3rd edition, (London: Athlone)
- Allen, D. A., Hyland, A. R. & Hillier, D. J. 1990, *MNRAS*, 244, 706
- Becklin, E. E., Matthews, K., Neugebauer, G & Willner, S. P. 1978, *ApJ*, 219, 121
- Blum, R. D., Sellgren, K. & DePoy, D. L. 1995, *ApJ*, 440, L17
- Blum, R. D., DePoy, D. L. & Sellgren, K. 1995, *ApJ*, 441, 603
- Chlewbowski, T., & Garmany, C. D. 1991, *ApJ*, 368, 241
- Cohen, M. 1995, *ApJS*, 100, 413
- Conti, P. S. 1984, in *IAU Symp. 105, Observational Tests of Stellar Evolution Theory*, eds. A. Maeder & A. Renzini (Dordrecht: Reidel), 233
- Cotera, A. S., Erickson, E. F., Colgan, S. W. J., Simpson, J. P., Allen, D. A., & Burton, M. G. 1996, *ApJ*, 461, 750
- Crowther, P. A., & Smith, L. J. 1996, *A&A*, 305, 541
- Drissen, L., Moffat, A. F. J., Walborn, N. R., & Shara, M. M. 1995, *AJ*, 110, 2235
- Egan, M. P., Shipman, R. F., Price, S. D., Carey, S. J., Clark, F. O., & Cohen, M. 1998, *ApJ*, 494, L199
- Eisenhauer, F., Quirrenbach, A., Zinnecker, H., & Genzel, R. 1998, *ApJ*, 498, 278
- Elias, J. H.; Frogel, J. A.; Matthews, K.; Neugebauer, G. 1982, *AJ*, 87, 1029
- Figer, D. F. 1995, PhD Thesis, University of California, Los Angeles
- Figer, D. F. 1996, in *Workshop on the Quintuplet, Pistol, and Sickle*, held at UCLA, September, 1996.
- Figer, D. F., McLean, I. S. & Morris, M. 1995, *ApJ*, 447, L29
- Figer, D. F., McLean, I. S., Morris, M., & Najarro, F. 1998a, in *The Central Regions of the Galaxy and Galaxies*, IAU No. 184, in press
- Figer, D. F., McLean, I. S., & Najarro, F. 1997, *ApJ*, 486, 420
- Figer, D. F., Morris, M., & McLean 1996, in *ASP Conf. Ser. 102, The Galactic Center, 4th ESO/CTIO Workshop*, ed. R. Gredel (San Francisco: ASP), 263
- Figer, D. F., Najarro, F., Morris, M., McLean, I. S., Geballe, T. R., Ghez, A. M., & Langer, N. 1998b, *ApJ*, 506, 384
- Figer, D. F., et al. 1999, in preparation
- Geballe, T. R., Genzel, R., Krabbe, A., Krenz, T. & Lutz, D. 1994, in *Infrared Astronomy with Arrays*, ed. I. S. McLean (Dordrecht: Kluwer), 73
- Genzel, R., Thatte, N., Krabbe, A., Kroker, H. & Tacconi-Garman 1996, *ApJ*, 472, 153
- Glass, I. S., Catchpole, R. M., & Whitelock, P. A. 1987, *MNRAS*, 227, 373
- Glass, I. S., Moneti, A. & Moorwood, A. F. M. 1990, *MNRAS*, 242, 55P
- Habing, H. J., Olmon, R. M., Winnberg, A., Matthews, H. E., & Baud, B. 1983, *A&A*, 128, 230
- Hanson, M. M., Conti, P. S. & Rieke 1996, *ApJS*, 107, 281
- Harris, A. I., Krenz, T., Genzel, R., Krabbe, A., Lutz, D., Poglitsch, A., Townes, C. H. & Geballe, T. R. 1994, in *The Nuclei of Normal Galaxies: Lessons from the Galactic Center*, eds. R. Genzel & A. I. Harris (Dordrecht: Kluwer), 223
- Ho, L. C., & Filippenko, A. V. 1996, *ApJ*, 472, 600
- Kennicutt, R. C. 1984, *ApJ*, 287, 116

- Koornneef, J. 1983, *A&A*, 128, 84
- Krabbe, A., Genzel, R., Drapatz, S. & Rotaciuc, V. 1991, *ApJ*, 382, L19
- Krabbe, A., et al. 1995, *ApJ*, 447, L95
- Lang, C. C., Goss, W. M., & Wood, D. O. S. 1997, *ApJ*, 474, 275
- Lasenby, J., Lasenby, A. N., & Yusef-Zadeh, F. 1989, *ApJ*, 343, 177
- Levine, D., Morris, M., & Figer, D. F. 1999, in *Proceedings of The Universe as Seen by ISO*, ESA Special Publications series (SP-427), in press
- Libonate, S., Pipher, J. L., Forrest, W. J., & Ashby, M. L. N. 1995, *ApJ*, 439, 202
- Massey, P., & Hunter, D. A. 1998, *ApJ*, 493, 180
- McCaughrean, M. J., & Stauffer, J. R. 1994, *AJ*, 108, 1382
- McLean, I. S., et al. 1993, in *Infrared Detectors and Instrumentation*, ed. A. Fowler (Bellingham: SPIE), 513
- McLean, I. S., et al. 1994, in *Instrumentation in Astronomy VIII*, ed. D. Crawford (Bellingham: SPIE), 457
- Meynet, G., Maeder, A., Schaller, G., Schaerer, D., & Charbonnel, C. 1994, *A&A Supp.*, 103, 97
- Meynet, G. 1995, *A&A*, 298, 767
- Moffat, A. F. J., Drissen, L., & Shara, M. M. 1994, *ApJ*, 436, 183
- Moneti, A., Glass, I. S. & Moorwood, A. F. M. 1994, *MNRAS*, 268, 194
- Morris, M., Davidson, J. A., & Werner, M. W. 1995, in *ASP Conf. Ser. 73, Airborne Astronomy Symposium on the Galactic Ecosystem*, eds. M. R. Haas, J. A. Davidson, E. F. Erickson (San Francisco: ASP), 477
- Nagata, T., Woodward, C. E., Shure, M., Pipher, J. L. & Okuda, H. 1990, *ApJ*, 351, 83
- Nagata, T., Hyland, A. R., Straw, S. M., Sato, S., & Kawara, K. 1993, *ApJ*, 406, 501
- Nagata, T., Kobayashi, N., & Sato, S. 1994, *ApJ*, 423, L113
- Nagata, T., Woodward, C. E., Shure, M., & Kobayashi, N. 1995, *ApJ*, 109, 1676
- Najarro, F. 1995, PhD Thesis, Ludwig-Maximilian University
- Najarro, F., Krabbe, A., Genzel, R., Lutz, D., Kudritzki, R. P., & Hillier, D. J. 1997, *A&A*, 325, 700
- Okuda, H, Shibai, H., Nakagawa, T., Matsuhara, H., Kobayashi, Y., Kaifu, N., Nagata, T., Gately, I. & Geballe, T. R. 1990, *ApJ*, 351, 89
- Panagia, N. 1973, *AJ*, 78, 929
- Reid, M. J. 1993, *ARA&A*, 31, 345
- Rieke, G. H., Rieke, M. J., & Paul, A. E. 1989, *ApJ*, 336, 752
- Salpeter, E. E. 1955, *ApJ*, 121, 161
- Scalo, J. 1998, in *The Stellar Initial Mass Function (38th Herstmonceux Conference)*, eds. G. Gilmore, & D. Howell, (San Francisco: ASP), 201
- Sellgren, K. 1989, in *IAU Symp. 136, The Center of the Galaxy*, ed. M. Morris (Dordrecht: Kluwer), 477
- Serabyn, E., & Güsten, R. 1991, *A&A*, 242, 376
- Serabyn, E., & Morris, M. 1994, *ApJ*, 424, L91
- Serabyn, E., Shupe, D., & Figer, D. F. 1998, *Nature*, in press
- Shipman, R. F., Egan, M. P., & Price, S. D. 1996, *BAAS*, 189, 61.04
- Simpson, J. P., Colgan, S. W. J., Cotera, A. S., Erickson, E. F., Haas, M. R., Morris, M., & Rubin, R. H. 1997, *ApJ*, 487, 689
- Sjouwerman, L. O., Van Langevelde, H. J., Winnberg, A., & Habing, H. J. 1998, *A&AS*, 128, 35

Stahler, S. W. 1994, *PASP*, 106, 337

Tamblyn, P., Rieke, G. H., Hanson, M. M., Close, L. M., McCarthy, D. W., Jr., & Rieke, M. J. 1996, *ApJ*, 456, 206

Timmermann, R., Genzel, R., Poglitsch, A., Lutz, D., Madden, S. C., Nikola, T., Geis, N. & Townes, C. H. 1996, *ApJ*, 466, 242

Vacca, W. D., Garmany, C. D., & Shull, J. M. 1996, *ApJ*, 460, 914

van der Hucht, K. A., Conti, P. S., Lundström, I., & Stenholm, B. 1981, *Space Sci. Rev.*, 28, 227

Wainscoat, R. J. & Cowie, L. L. 1992, *AJ*, 103, 332

Walborn, N. R. 1991, in *IAU Symp. 148, The Magellanic Clouds*, ed. R. Haynes & D. Milne (Dordrecht: Kluwer), 145

Williams, P. M., van der Hucht, K. A. & Thé, P. S. 1987, *A&A*, 182, 91

Winnberg, A., Baud, B., Matthews, H. E., Habing, H. J., & Olton, F. M. 1985, *ApJ*, 291, L45

Yusef-Zadeh, F., & Morris, M. 1987, *AJ*, 94, 1178

Yusef-Zadeh, F., Morris, M. & van Gorkom, J. H. 1989, in *IAU Symp. 136, The Center of the Galaxy*, ed. M. Morris (Dordrecht: Kluwer), 275

Fig. 1.— JHK' color composite of the Quintuplet Cluster, covering $3' \times 3'$.

Fig. 2a.— J-band image of Quintuplet Cluster, covering $3' \times 3'$.

Fig. 2b.— H-band image of Quintuplet Cluster, covering $3' \times 3'$.

Fig. 2c.— K'-band image of Quintuplet Cluster, covering $3' \times 3'$.

Fig. 2d.— nbL-band image of Quintuplet Cluster, covering $3' \times 3'$. The diagonal lines are artifacts from bad pixels in the array.

Fig. 3a.— Alternate stretch of Figure 2c at an expanded scale with respect to Figures 1-2.

Fig. 3b.— Schematic diagram of the stars covered in the slit-scan. Individual stars are labeled with number according to Table 1. The slit-scan did not include stars #353e and #362.

Fig. 4.— Identified spectral types in the Quintuplet Cluster. The slit-scan area is shown as a rectangular box. See text for a description of how the stellar types were determined.

Fig. 5.— K-band spectra of WR stars in the Galaxy obtained with the same instrument and setup as was used to obtain the target spectra in this paper ($R \approx 525$). The identification numbers are taken from van der Hucht et al. (1981). WC stars are shown in the left panels, and WN stars are shown in the right panels. Likely emission line identifications are indicated by tick marks.

Fig. 6a.— K-band spectra of WN9 stars in the Quintuplet and WR108 (WN9). Features near $2.05 \mu\text{m}$, $2.315 \mu\text{m}$, and $2.370 \mu\text{m}$, are

This 2-column preprint was prepared with the AAS L^AT_EX macros v4.0.

suspect due to difficulties in correcting for atmospheric absorption; tick marks indicate that features at these wavelengths are uncertain. All subsequent spectra have been dereddened according to the text.

Fig. 6b.— K-band spectra of #353e (WN6) in the Quintuplet and WR115 (WN6). See caption for Figure 6a for more.

Fig. 6c.— K-band spectra of #76 (WC9) in the Quintuplet and WR121 (WC9).

Fig. 6d.— K-band spectra of WC8 and “₁WC8” stars in the Quintuplet and WR135 (WC8). We have used measurements of the excess emission at 3.09 μm He II lines to classify the “<WC8” stars. See caption for Figure 6a for more.

Fig. 7.— K-band spectra of OB supergiants in the Quintuplet. In cases where two spectra are shown, the upper spectrum was taken on the earlier date. A curve for a hot blackbody has been overplotted for comparison. The “<B0I” stars have nearly featureless spectra which can only be matched to spectra of stars earlier than B0I. The “OBI” stars have an ambiguous classification, showing a hint of absorption in the 2.112 μm He I line and the 2.166 μm H I line with a small amount of excess emission in the 2.058 μm He I line in some cases. The dereddened spectra are steeper than the blackbody curve in some cases, i.e., #270S. Evidently, $A_K = 3.2$ is too high for this star. Note the lack of CO absorption features, i.e., at 2.294 μm , in the spectrum for #362 (see text). See caption for Figure 6a for more.

Fig. 8.— K-band spectra of early B supergiants in the Quintuplet. In cases where two spectra are shown, the upper spectrum was

taken on the earlier date. A curve for a hot blackbody has been overplotted for comparison. Features at 2.312 μm and 2.370 μm are due to imperfect atmospheric correction. The spectra for #311 and #344 have low signal-to-noise. The August 20, 1996, spectrum of #311 reveals a late-type companion as seen in the CO absorption features longward of 2.29 μm . See caption for Figure 6a for more.

Fig. 9a.— Dereddened spectral energy distribution of #243 (#1 in MGM94). We assume $A_K = 2.7$ because this value gives the best fit between the observations and the blackbodies. A best-fit blackbody curve has been overplotted here and in Figures 9b-e.

Fig. 9b.— Dereddened spectral energy distribution of #231 (#2 in MGM94). See Figure 9a for more.

Fig. 9c.— Dereddened spectral energy distribution of #211 (#3 in MGM94). See Figure 9a for more.

Fig. 9d.— Dereddened spectral energy distribution of #251 (#4 in MGM94). See Figure 9a for more.

Fig. 9e.— Dereddened spectral energy distribution of #258 (#9 in MGM94). See Figure 9a for more.

Fig. 10.— K-band spectra of two stars near the Quintuplet. The spectra are well-fit by cool blackbody curves. See caption for Figure 6a for more.

Fig. 11.— Model isochrones from the Geneva models for $Z = 0.04$ with “2 \times ” mass-loss. Isochrones begin at 1 Myr and are spaced by 1 Myr. Data for early B supergiants in the Quintuplet Cluster are overplotted. The error in temperature covers the range for B1I–B3I

stars. The error in luminosity is dominated by errors in determining the extinction. Assuming that the upper data points are influenced by confusion or binarity, we find a cluster age ≈ 4 Myr.

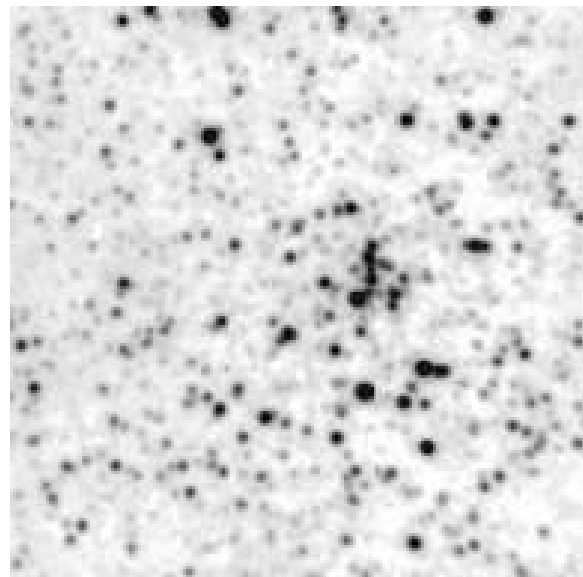


Figure 2a

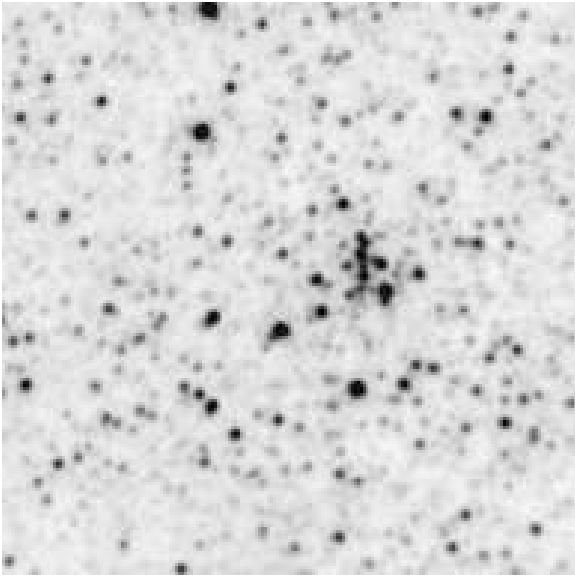


Figure 2b

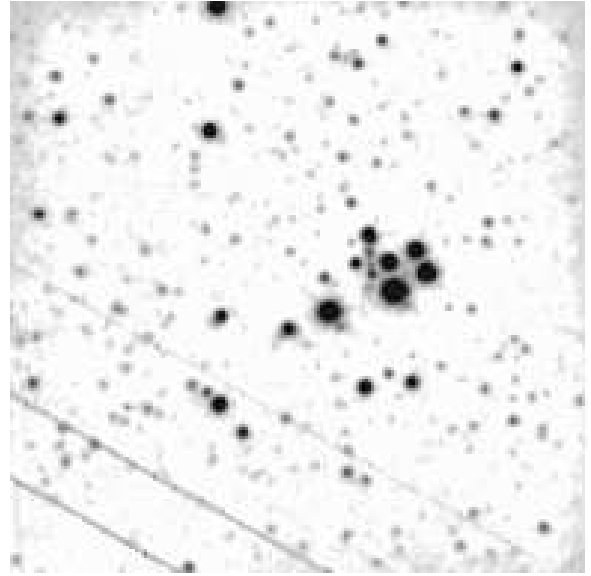


Figure 2d

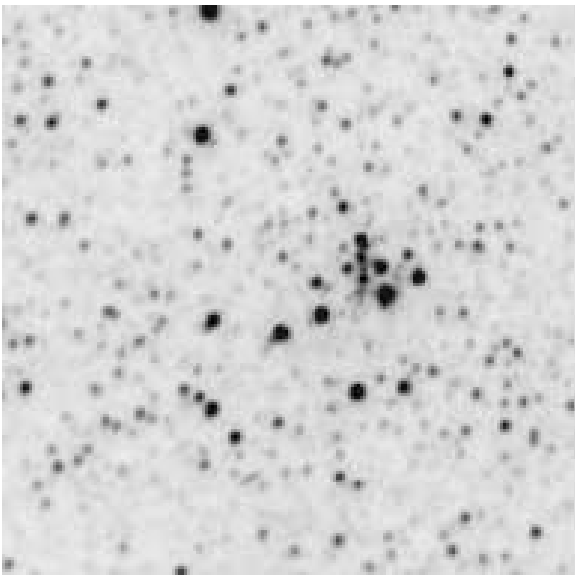


Figure 2c

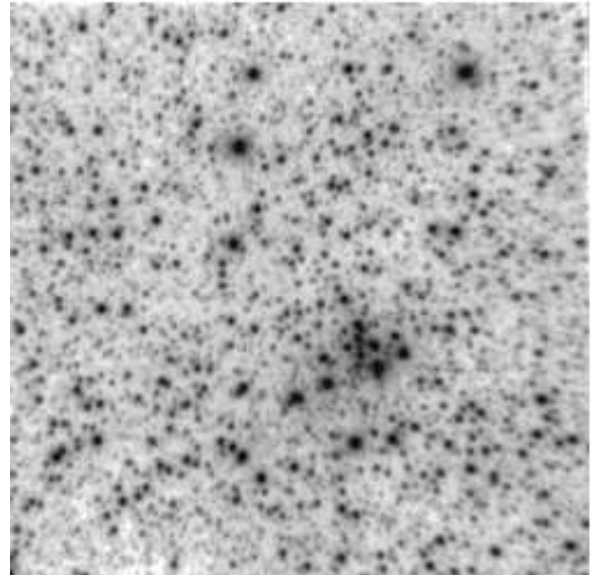


Figure 3a

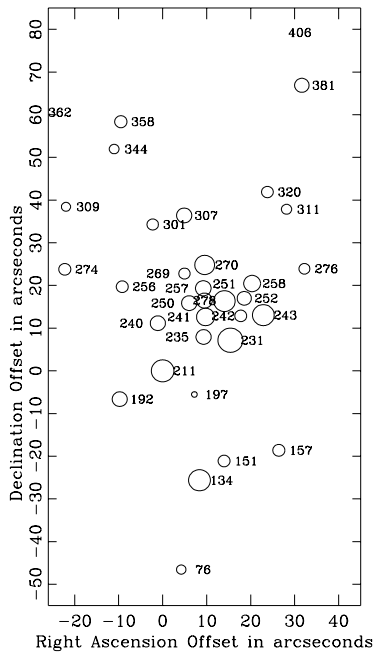


Figure 3b

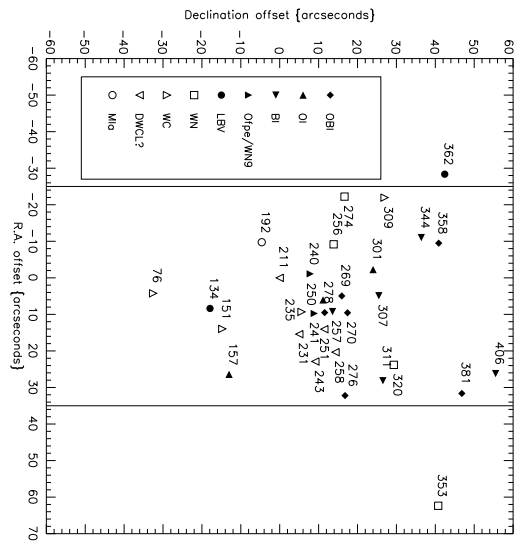


Figure 4

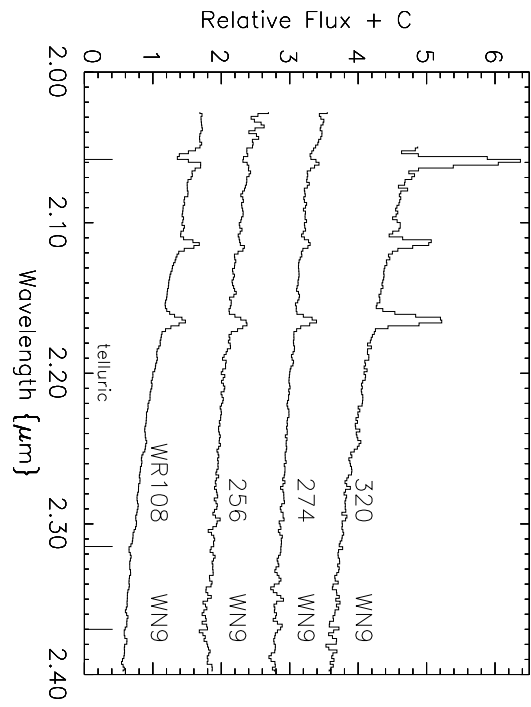


Figure 6a

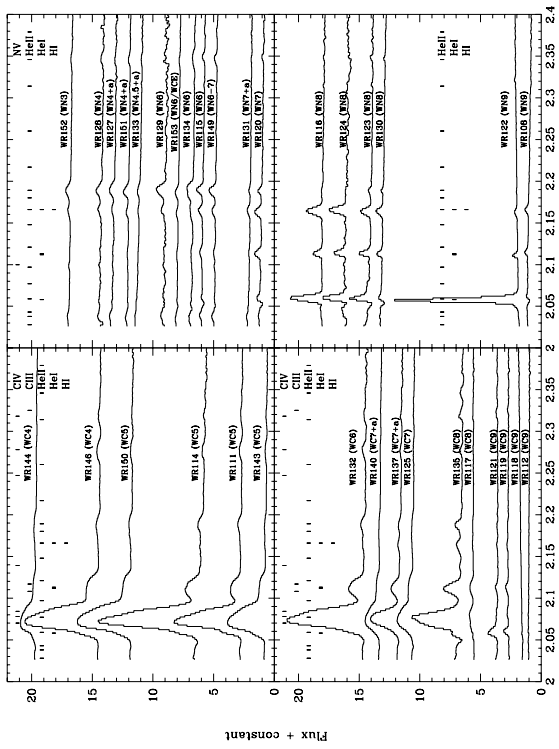


Figure 5

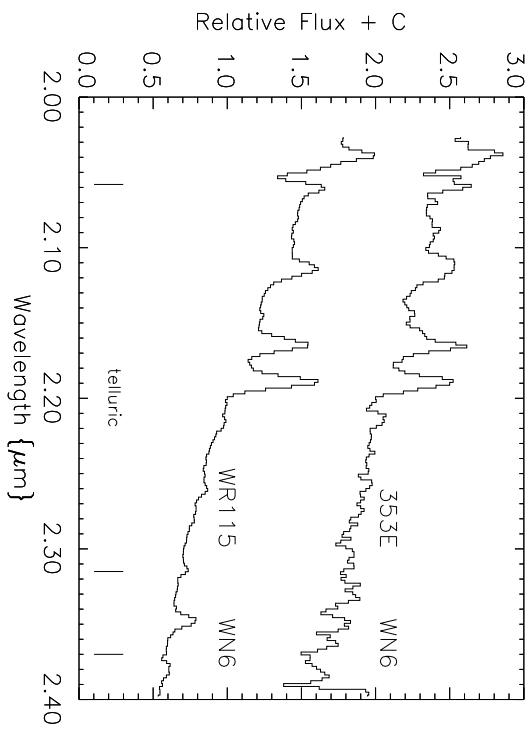


Figure 6b

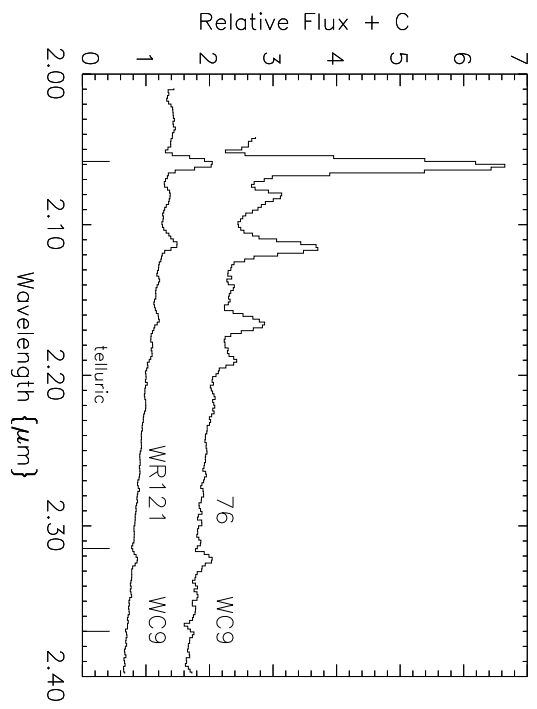


Figure 6c

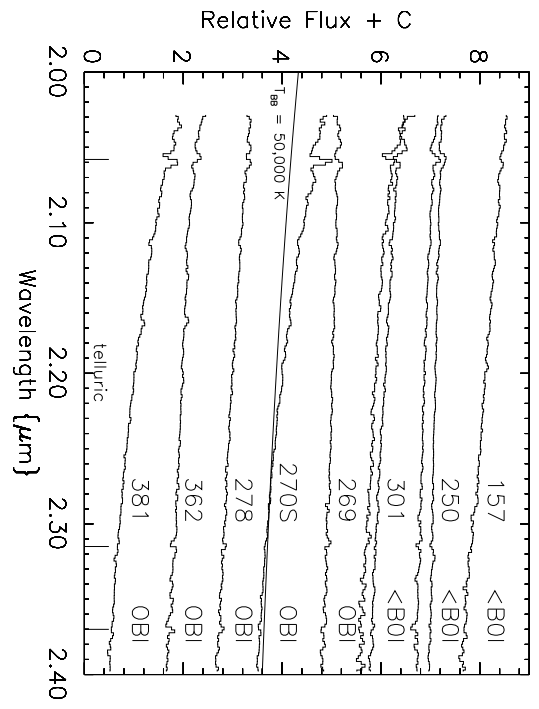


Figure 7

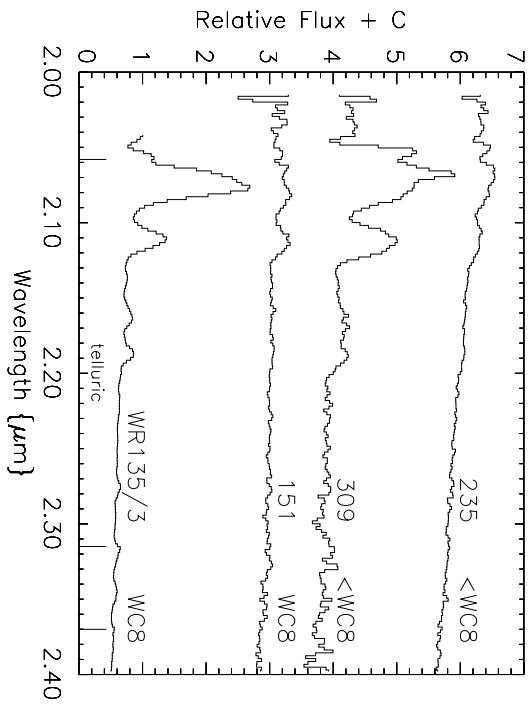


Figure 6d

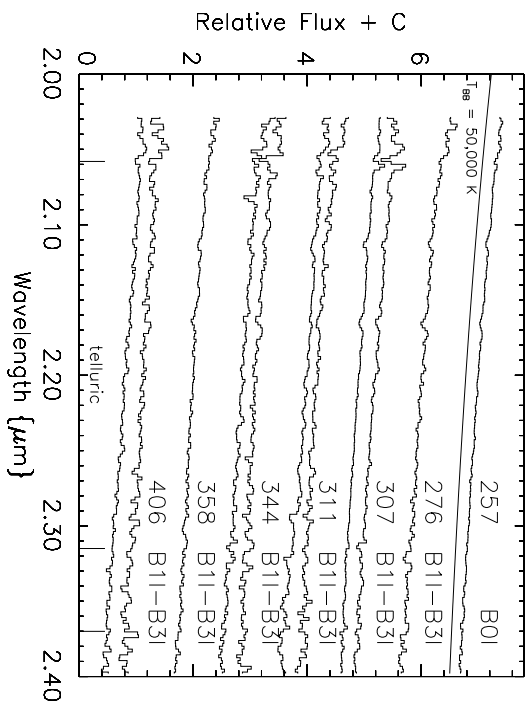


Figure 8

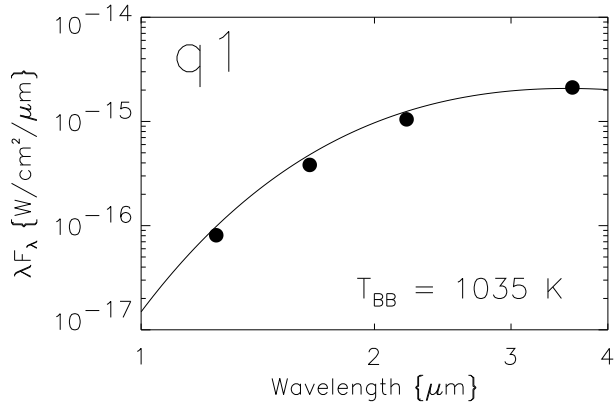


Figure 9a

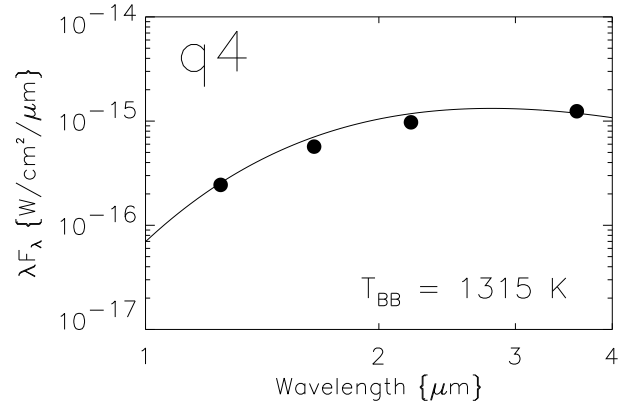


Figure 9d

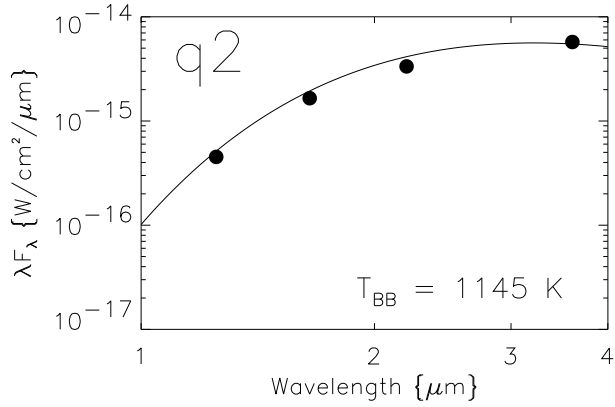


Figure 9b

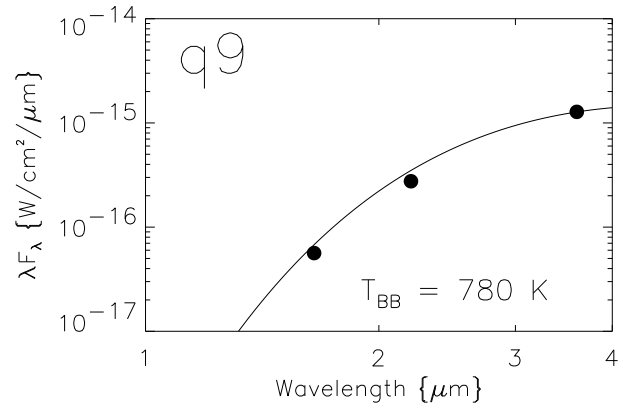


Figure 9e

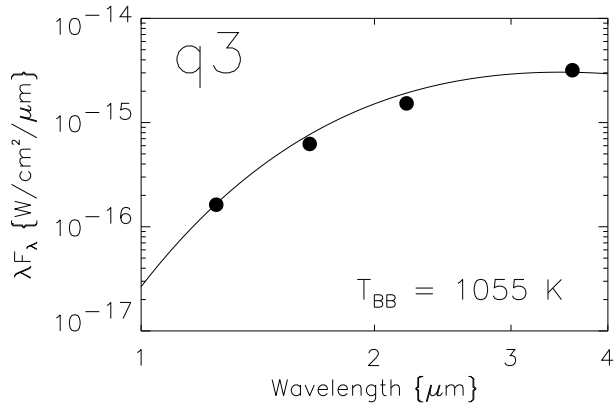


Figure 9c

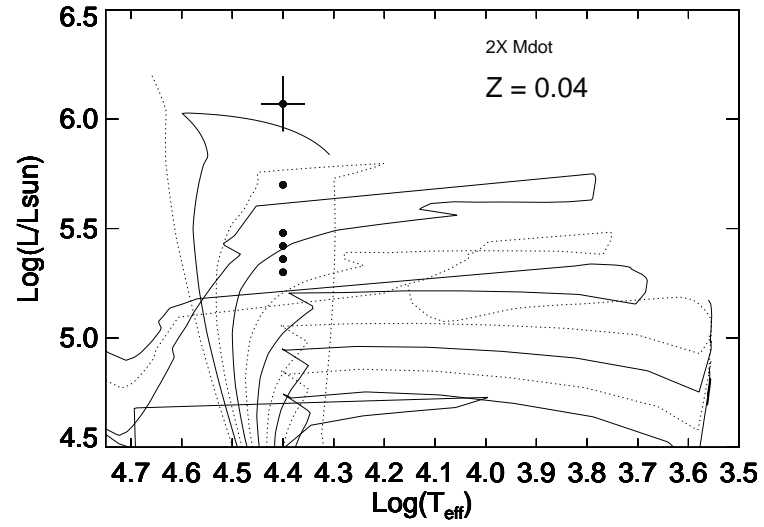


Figure 11

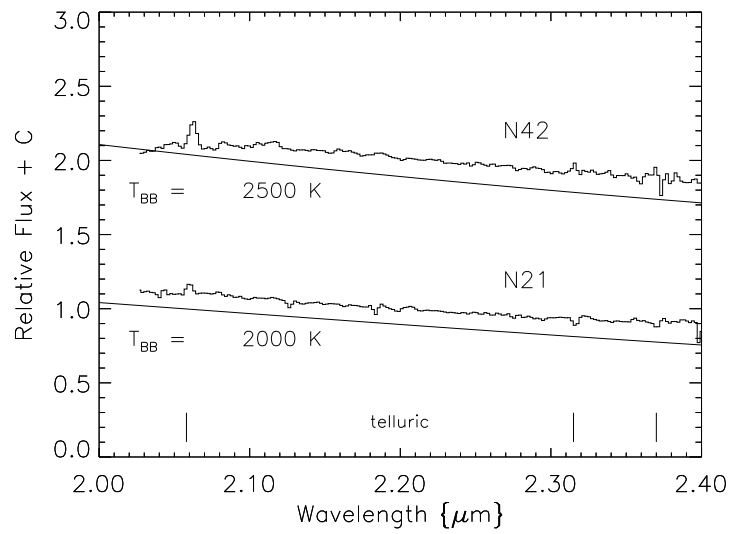


Figure 10